Alternating-current response of one-dimensional quantum dot arrays

2002 J. Phys.: Condens. Matter 14 703

(http://iopscience.iop.org/0953-8984/14/4/305)

INSTITUTE OF PHYSICS PUBLISHING JOURNAL OF PHYSICS: CONDENSED MATTER

J. Phys.: Condens. Matter **14** (2002) 703–713 PII: S0953-8984(02)30313-8

Alternating-current response of one-dimensional quantum dot arrays

Yabin Yu[1,2], **T C Au Yeung**[1], **W Z Shangguan**[1] **and C H Kam**[1]

[1] School of Electrical and Electronic Engineering, Nanyang Technological University, 639798, Singapore
[2] Department of Physics, Yantai University, Yantai 264005, People's Republic of China

Received 31 October 2001
Published 18 January 2002
Online at stacks.iop.org/JPhysCM/14/703

Abstract

A general approach is presented for calculating the dynamic conductance of coupled quantum dot systems. To consider the long-range Coulomb interaction, we introduce the capacitances between the leads and dots, gate electrodes and dots, and dots and dots. The displacement currents are also taken into account. Our results fulfil charge and current conservation requirements, as well as current and charge response invariance under an overall potential shift. We apply our approach to a one-dimensional quantum dot array by use of the non-equilibrium Green function techniques. The numerical results are presented for a three-quantum-dot system. Three-peak resonant structure of the alternating-current conductance is observed at low temperature. The effect of the capacitance on the frequency-dependent conductance is obvious, but less so at low frequency. The low-frequency conductance shows either capacitive or inductive behaviour depending on the chemical potential of the electron reservoirs, but sufficiently large capacitances may change this situation.

1. Introduction

Alternating-current transport properties of mesoscopic conductor systems have attracted much research attention, both experimental [1–3] and theoretical [4–18]. In recent years, many studies of quantum dot (QD) systems consisting of coupled dots have appeared in the literature [8–16, 19–25]. Büttiker *et al* [9–11] have published much work discussing the ac response of mesoscopic systems. In [9], using discrete-potential models, they studied the dynamic conductance of QD systems with a number of dots and leads (contacts), in which it was assumed that no tunnelling occurs between the dots. However, in most situations, the systems involved tunnel couplings between the QDs. In this paper, we extend the idea of Büttiker *et al* [9] to systems with inter-dot tunnelling, and develop a general approach for calculating the frequency-dependent conductance of the coupled QD systems. As an example, we apply our approach to a one-dimensional (1D) coupled QD array, and, with the help of the

non-equilibrium Green function techniques, present a calculation of the frequency-dependent conductance.

2. General theory for the response of coupled QD systems

For general purposes, we first consider a system of N tunnel-coupled QDs, which are connected with a number of contacts (electron reservoirs) via tunnel coupling. The gate electrodes are included in the system as electron reservoirs, which have no tunnelling connections to the QDs, but are coupled capacitively with the QDs. Alternating fields are applied to the electron reservoirs in addition to dc voltages. This system can be described by the following model Hamiltonian:

$$H = \sum_i \sum_{\alpha_i,k} \epsilon_{ks\alpha_i}(t) c^\dagger_{ks\alpha_i} c_{ks\alpha_i} + \sum_{i,n} \epsilon_{i,n}(t) d^\dagger_{in} d_{in} + \sum_{n,m,i<j} (V_{im,jn} d^\dagger_{im} d_{jn} + \text{h.c.}) + \sum_i \sum_{k,n,\alpha_i} (V_{ks\alpha_i,n} c^\dagger_{ks\alpha_i} d_{in} + \text{h.c.}) \tag{1}$$

where $c^\dagger_{ks\alpha_i}$ ($c_{ks\alpha_i}$) is the creation (annihilation) operator for an electron with momentum k in channel s of reservoir α_i connected to dot i, $d^\dagger_{in}$ (d_{in}) is the electron creation (annihilation) operator for the nth level in dot i, $V_{im,jn}$ is the tunnelling coupling between the two dots, and $V_{ks\alpha_i,n}$ is the tunnelling coupling between nth level in dot i and reservoir α_i. Applying a time-dependent potential $V_{\alpha_i}(t)$ to the contact α_i causes the electron energy in the contact to vary as $\epsilon_{ks\alpha_i}(t) = \epsilon_{ks\alpha_i} + eV_{\alpha_i}(t)$, and this ac potential results in a time-dependent energy in the dots: $\epsilon_{in}(t) = \epsilon^0_{in} + eV_i(t)$, where $V_i(t)$ is the so-called internal potential. In this model we do not introduce the many-body terms describing interaction between electrons; instead we describe the interaction by the effective potential seen by the interacting electrons. This is in fact a mean-field picture. In this model, the ac tunnelling current from reservoir α_i into dot i is given by

$$I^{\text{Tun}}_{\alpha_i}(t) = \frac{e}{\hbar} \sum_{ks\in\alpha_i,n} [\text{i}V_{ks\alpha_i,n} \langle c^\dagger_{ks\alpha_i} d_{in}(t)\rangle + \text{c.c.}]. \tag{2}$$

According to linear-response theory, for Hamiltonian (1) we obtain the following Kubo-like formula for the ac current response to small ac voltages and internal potentials:

$$\delta I^{\text{Tun}}_{\alpha_i}(t) = \int \sigma_{\alpha_i,I}(t-t') V_I(t')\,\text{d}t' \tag{3}$$

where $\sigma_{\alpha_i,I}(t-t') = -\text{i}\theta(t-t')\langle[\hat{I}_{\alpha_i}(t), e\hat{N}_I(t')]\rangle_0$ is the tunnelling current operator, and $\hat{I}_{\alpha_i}(t) = (e/\hbar)\sum_{ks\in\alpha_i,n}[\text{i}V_{ks,n} c^\dagger_{ks\alpha_i}(t) d_{in}(t) + \text{h.c.}]$. Here $\langle\cdots\rangle_0$ represents the mean value for the system without time-dependent perturbation. $\hat{N}_I$ is the number operator for the electrons in the contacts or QDs, and the label $I = \{\alpha_i, i\}$. The frequency-dependent current is then obtained from equation (3)

$$\delta I^{\text{Tun}}_{\alpha_i}(\omega) = \sum_I \sigma^{\text{Tun}}_{\alpha_i,I}(\omega) V_I(\omega) \tag{4}$$

where the tunnelling conductance $\sigma^{\text{Tun}}_{\alpha_i,I}(\omega) = \int \sigma_{\alpha_i,I}(t)\text{e}^{-\text{i}\omega t}\,\text{d}t$ is the Fourier transform of the correlation function $\sigma_{\alpha_i,I}(t)$. It is worth pointing out that the expressions for the current (2) and the linear response (3) and (4) are general, and valid for models including interaction terms in the contacts and dots.

Our next job is to determine the internal potential $V_i(t)$. For this purpose, following Büttiker *et al* [9] we consider all conducting units (contacts and QDs) which interact via long-range Coulomb forces, and assume that all electric field lines from one of the QDs and contacts

terminates at the nearby QDs and contacts. Due to the tunnelling between them, charge piles up in contacts and QDs, and the pile-up charge in one dot or contact induces counterbalancing charge on the other dots or contacts. We consider the long-range Coulomb interaction by introducing formal geometrical capacitances C_{IJ} that relate the total charges Q_I in the QDs (i) or contacts (α_i) to the potentials (V_α and V_i):

$$Q_i = \sum_j C_{ij} V_{\alpha_j} + \sum_j \sum_{\alpha_j} C_{i\alpha_j} V_{\alpha_j} \tag{5}$$

and

$$Q_{\alpha_i} = \sum_j C_{\alpha_i j} V_j + \sum_j \sum_{\alpha_j} C_{\alpha_i \alpha_j} V_{\alpha_j} \tag{6}$$

with $C_{IJ} = C_{JI}$ ($I = i, \alpha_i$ and $J = j, \alpha_j$) and $\sum_J C_{IJ} = 0$. On the other hand, the charges Q_i in the QDs can be calculated via $\sum_n e\langle {d_{in}}^\dagger(t) d_{in}(t)\rangle$ by making use of Keldysh Green function techniques. Similar to the current response $\delta I^{\mathrm{Tun}}_{\alpha_i}$, we have the charge response in the QDs

$$\delta Q_i(\omega) = \sum_I e^2 N_{i,I}(\omega) V_I(\omega) \tag{7}$$

where $N_{i,I}(t) = -\mathrm{i}\theta(t)\langle[\hat{N}_i(t), \hat{N}_I(0)]\rangle_0$. From equations (5) and (7), the internal potentials are obtained:

$$\delta V_i(\omega) = \sum_k (M^{-1})_{ik}(\omega) \sum_j \sum_{\alpha_j} (e^2 N_{k\alpha_j}(\omega) - C_{k\alpha_j}) V_{\alpha_j}(\omega). \tag{8}$$

Consequently, we obtain the following total ac response

$$\delta I_{\alpha_i}(\omega) = \delta I^{\mathrm{Tun}}_{\alpha_i}(\omega) - \mathrm{i}\omega \delta Q_{\alpha_i}(\omega) = \sum_j \sum_{\alpha_j} \sigma_{\alpha_i \alpha_j}(\omega) V_{\alpha_j}(\omega) \tag{9}$$

and the true conductance

$$\begin{aligned}\sigma_{\alpha_i\alpha_j}(\omega) = {} & \sigma^{\mathrm{Tun}}_{\alpha_i\alpha_j}(\omega) + \sum_{k,l} \sigma^{\mathrm{Tun}}_{\alpha_i k}(\omega)(M^{-1})_{kl}(\omega)(e^2 N_{l\alpha_j}(\omega) - C_{l\alpha_j}) \\ & - \mathrm{i}\omega\left[C_{\alpha_i\alpha_j} + \sum_{k,l} C_{\alpha_i k}(M^{-1})_{kl}(\omega)(e^2 N_{l\alpha_j}(\omega) - C_{l\alpha_j})\right]\end{aligned} \tag{10}$$

where $M(\omega)$ is the following matrix:

$$M_{ij}(\omega) = C_{ij} - e^2 N_{ij}(\omega). \tag{11}$$

We show below that the conductance given by equation (10) satisfies overall current conservation:

$$\sum_i \sum_{\alpha_i} \sigma_{\alpha_i\alpha_j}(\omega) = 0 \tag{12}$$

and gauge invariance under an overall potential shift:

$$\sum_j \sum_{\alpha_j} \sigma_{\alpha_i\alpha_j}(\omega) = 0. \tag{13}$$

From equations (1) and (2), one can verify the charge conservation law [4, 18]

$$\sum_i e\dot{N}_i(t) = \sum_i \sum_{\alpha_i} I^{\mathrm{Tun}}_{\alpha_i}(t) \qquad \text{or} \qquad -\sum_i \mathrm{i}\omega e \delta N_i(\omega) = \sum_{\alpha_i} \delta I^{\mathrm{Tun}}_{\alpha_i}(\omega). \tag{14}$$

Combining equations (5)–(9) and (14) with $\sum_I C_{IJ} = 0$, one finds that the conductance equation (10) fulfils the overall current conservation requirement (12). On the other hand,

we notice that the current response of the system is invariant under the following canonical transformation [6]:

$$\bar{H} = U^{-1}HU - \mathrm{i}U^{-1}\frac{\partial}{\partial t}U \tag{15}$$

with $U = \exp\{\mathrm{i}\int_{-\infty}^{t} \mathrm{d}\bar{t}\,\Delta(\bar{t})[\sum_{ks\in\alpha_i} c^{\dagger}_{ks\alpha_i}c_{ks\alpha_i} + \sum_{i,n} d^{\dagger}_{in}d_{in}]\}$, where $\Delta(t)$ is an arbitrary function of t. This transformation performs an overall potential shift in Hamiltonian (1), i.e., $\epsilon_{ks\alpha_i}(t) \to \epsilon_{ks\alpha_i}(t) - \Delta(t)$ and $\epsilon_{i,n}(t) \to \epsilon_{i,n}(t) - \Delta(t)$. Therefore, the current response equation (2) fulfils invariance under an overall potential shift, and hence is a functional of $\epsilon_{ks\alpha_i}(t) - \Delta(t)$ and $\epsilon_{i,n}(t) - \Delta(t)$:

$$I^{\mathrm{Tun}}_{\alpha_i}(t) = I^{\mathrm{Tun}}_{\alpha_i}(\{\epsilon_{ks\alpha_i}(t), \epsilon_{i,n}(t)\}, t) = I^{\mathrm{Tun}}_{\alpha_i}(\{\epsilon_{ks\alpha_i}(t) - \Delta(t), \epsilon_{i,n}(t) - \Delta(t)\}, t) \tag{16}$$

for any $\Delta(t)$. Property (12) is therefore obtained from the combination of (16) and $\sum_J C_{IJ} = 0$ with the other related equations.

3. Formulae for the conductance of the 1D QD array

Equation (3) is valid for general systems, even ones including interaction of electrons in the contacts. However, for our case, where there is no interaction term in the Hamiltonian, the ac tunnelling current flowing from the α_i-reservoir into dot i can be calculated using the Keldysh Green functions

$$\begin{aligned} I^{\mathrm{Tun}}_{\alpha_i}(t) = \frac{e}{\hbar}\,\mathrm{Tr}\int \mathrm{d}t_1\,\{&\boldsymbol{G}^r_i(t,t_1)\boldsymbol{\Sigma}^<_{\alpha_i}(t_1,t) + \boldsymbol{G}^<_i(t,t_1)\boldsymbol{\Sigma}^a_{\alpha_i}(t_1,t) \\ &- \boldsymbol{\Sigma}^<_{\alpha_i}(t,t_1)\boldsymbol{G}^a_i(t_1,t) - \boldsymbol{\Sigma}^r_{\alpha_i}(t,t_1)\boldsymbol{G}^<_i(t_1,t)\} \end{aligned} \tag{17}$$

where

$$[\boldsymbol{G}^<_i(t)]_{mn} = \mathrm{i}\langle d^{\dagger}_{in}(t')d_{im}(t)\rangle \tag{18}$$

$$[\boldsymbol{G}^r_i(t)]_{mn} = -\mathrm{i}\theta(t)\langle\{d_{im}(t),\ d^{\dagger}_{in}(t')\}\rangle \tag{19}$$

and the tunnelling self-energies are related to the free-particle Green functions ($g^{r,a,<}_{k\alpha_i}$) in the electron reservoirs and the tunnel couplings ($V_{ks\alpha_i,n}$) between the contacts and dots:

$$[\boldsymbol{\Sigma}^{r,a,<}_{\alpha_i}(t,t')]_{mn} = V^*_{\alpha_i m}V_{\alpha_i n}\sum_{ks\in\alpha_i} g^{r,a,<}_{ks\alpha_i}(t,t') \tag{20}$$

and

$$\begin{aligned} g^{r,a}_{ks\alpha_i}(t,t') &= \mp\mathrm{i}\theta\left(\pm t \mp t'\right)\exp\left[-\mathrm{i}\int_{t'}^{t}\mathrm{d}t_1\,\epsilon_{ks\alpha_i}(t_1)\right] \\ g^<_{ks\alpha_i}(t,t') &= \mathrm{i}f(\epsilon_{ks\alpha_l})\exp\left[-\mathrm{i}\int_{t'}^{t}\mathrm{d}t_1\,\epsilon_{ks\alpha_l}(t_1)\right] \end{aligned} \tag{21}$$

where $f(\epsilon)$ is the Fermi distribution function. The ac current response can then be obtained by linearizing the Green functions in equation (17) with respect to the time-dependent potentials

$$\begin{aligned} \delta I^{\mathrm{Tun}}_{\alpha_i}(\omega) = \frac{e}{\hbar}\,\mathrm{Tr}\int\frac{\mathrm{d}E}{2\pi}\,\mathrm{i}\boldsymbol{\Gamma}_{\alpha_i}(E)\Bigg\{&\left[\frac{f_{\alpha_i}(E) - f_{\alpha_i}(E+\omega)}{\omega}\right] \\ &\times\left[\boldsymbol{G}^r_i(E+\omega) - (\boldsymbol{G}^r_i(E))^*\right]eV_{\alpha_i}(\omega) \\ &+ f_{\alpha_i}(E)[\delta\boldsymbol{G}^r_i(E+\omega,E) - (\delta\boldsymbol{G}^r_i(E-\omega,E))^*] + \delta\boldsymbol{G}^<_i(E+\omega,E)\Bigg\} \end{aligned} \tag{22}$$

where $\delta\boldsymbol{G}$ are the linearized Green functions and $(\boldsymbol{\Gamma}_{\alpha_i})_{mn} = \sum_{ks\in\alpha_i} V_{ks\alpha_i,m}V^*_{ks\alpha_i,n}\delta(E - \epsilon_{ks\alpha_l})$ is the resonant width for contact α_i.

Up to here our discussion has been general, and valid for arbitrary tunnel-coupled QD systems. As an example, we next consider a 1D tunnel-coupled QD array with two ends connected to two leads (L and R) via tunnelling. The dots and contacts are in series, coupled capacitively, and the dots in the array are also coupled capacitively to a common gate electrode with an ac voltage $V_g(t)$. For simplicity, we use the wide-band approximation for the electronic structure of the contacts [4]. We therefore obtain the linearized Green functions

$$\delta \boldsymbol{G}_i^r(E+\omega, E) = \sum_i \bar{\boldsymbol{G}}_{ij}^r(E+\omega, E)(eV_j(\omega)) \tag{23}$$

and

$$\delta \boldsymbol{G}_i^<(E+\omega, E) = \sum_j \{\bar{\boldsymbol{G}}_{ij}^<(E+\omega, E) - [\bar{\boldsymbol{G}}_{ij}^<(E, E+\omega)]^*\} eV_j(\omega) + \sum_{\alpha=L,R} \{\bar{\boldsymbol{G}}_{i\alpha}^<(E+\omega, E) - [\bar{\boldsymbol{G}}_{i\alpha}^<(E, E+\omega)]^*\} eV_\alpha(\omega). \tag{24}$$

Equations (23) and (24) and the components $\bar{\boldsymbol{G}}_{ij(\alpha)}^{r,<}$ in them can be obtained by linearizing the following Dyson equations of path Green functions:

$$G_i(\tau, \tau') = g_i(\tau, \tau') + \int_c \mathrm{d}\tau_1 \, \mathrm{d}\tau_2 \, g_i(\tau, \tau_1)\Sigma_i(\tau_1, \tau_2)G_i(\tau_2, \tau') \tag{25}$$

$$\Sigma_i(\tau_1, \tau_2) = |V_{i-1\,i}|^2 \, G_{L,i-1}^0(\tau_1, \tau_2) + |V_{i\,i+1}|^2 \, G_{R,i+1}^0(\tau_1, \tau_2) \tag{26}$$

where

$$G_{L,i}^0(\tau, \tau') = g_i(\tau, \tau') + |V_{i-1\,i}|^2 \int_c \mathrm{d}\tau_1 \, \mathrm{d}\tau_2 \, g_i(\tau, \tau_1)G_{L,i-1}^0(\tau_1, \tau_2)G_{L,i}^0(\tau_2, \tau') \quad \text{for } i = 2, 3, \ldots, N \tag{27}$$

$$G_{L,1}^0(\tau, \tau') = g_1(\tau, \tau') + \int_c \mathrm{d}\tau_1 \, \mathrm{d}\tau_2 \, g_1(\tau, \tau_1)\Sigma_L(\tau_1, \tau_2)G_{L,1}^0(\tau_2, \tau') \tag{28}$$

$$G_{R,i}^0(\tau, \tau') = g_i(\tau, \tau') + |V_{i\,i+1}|^2 \int_c \mathrm{d}\tau_1 \, \mathrm{d}\tau_2 \, g_i(\tau, \tau_1)G_{R,i+1}^0(\tau_1, \tau_2)G_{R,i}^0(\tau_2, \tau') \quad \text{for } i = 1, 2, \ldots, N-1 \tag{29}$$

and

$$G_{R,N}^0(\tau, \tau') = g_1(\tau, \tau') + \int_c \mathrm{d}\tau_1 \, \mathrm{d}\tau_2 \, g_1(\tau, \tau_1)\Sigma_R(\tau_1, \tau_2)G_{R,N}^0(\tau_2, \tau'). \tag{30}$$

Using equations (22)–(24) and related equations in the last section, we obtain the conductance of the 1D QD array:

$$\sigma_{\alpha\beta}(\omega) = \sigma_{\alpha\beta}^{\mathrm{Tun}}(\omega) + \sum_{ij} \sigma_{\alpha i}^{\mathrm{Tun}}(\omega)(M^{-1})_{ij}(\omega)(e^2 N_{j\beta}(\omega) - C_{j\beta}) - \mathrm{i}\omega C_\alpha \left[\delta_{\alpha\beta} - \sum_j (M^{-1})_{i_\alpha j}(\omega)(e^2 N_{j\beta}(\omega) - C_{j\beta})\right] \tag{31}$$

with

$$\sigma_{\alpha j}^{\mathrm{Tun}}(\omega) = \mathrm{i}\frac{e^2}{\hbar} \, \mathrm{Tr} \int \frac{\mathrm{d}E}{2\pi} \, \Gamma_\alpha \{f_\alpha(E)\bar{\boldsymbol{G}}_{i_\alpha j}^r(E+\omega, E) + \bar{\boldsymbol{G}}_{i_\alpha j}^<(E+\omega, E)\} + \mathrm{c.c.}(\omega \longrightarrow -\omega) \tag{32}$$

$$\sigma_{\alpha\beta}^{\mathrm{Tun}}(\omega) = \mathrm{i}\frac{e}{\hbar} \, \mathrm{Tr} \int \frac{\mathrm{d}E}{2\pi} \, \Gamma_\alpha \left\{\left[\frac{f_\alpha(E) - f_\alpha(E+\omega)}{\omega}\right] \boldsymbol{G}_{i_\alpha}^r(E+\omega)\delta_{\alpha\beta} + \bar{\boldsymbol{G}}_{i_\alpha\beta}^<(E+\omega, E)\right\} + \mathrm{c.c.}(\omega \longrightarrow -\omega) \tag{33}$$

and

$$N_{ij}(\omega) = -\mathrm{i}\int \frac{\mathrm{d}E_1}{2\pi}\,\mathrm{Tr}\{\bar{\boldsymbol{G}}^{<}_{ij}(E+\omega, E)\} + \text{c.c.}(\omega \longrightarrow -\omega) \tag{34}$$

$$N_{i\alpha}(\omega) = -\mathrm{i}\int \frac{\mathrm{d}E_1}{2\pi}\,\mathrm{Tr}\{\bar{\boldsymbol{G}}^{<}_{i\alpha}(E+\omega, E)\} + \text{c.c.}(\omega \longrightarrow -\omega) \tag{35}$$

where $\alpha, \beta = L, R$, and $i_\alpha = 1$ or N for $\alpha = L$ or R, respectively. The symbol c.c.$(\omega \to -\omega)$ means that we change ω to $-\omega$ in the first terms of the equations and then take the complex conjugate. Here $\sigma_{\alpha\beta}(\omega)$ is defined according to $\delta I_\alpha(\omega) = \sum_\beta \sigma_{\alpha\beta}(\omega)[V_\beta(\omega) - V_{\mathrm{g}}(\omega)]$. In equation (31) we have used the nearest-neighbour capacitance approximation

$$C_{ij} = \begin{cases} C_{i-1} + C_i + C_{\mathrm{g}}^{(i)} & j = i \\ -C_{i-1} & j = i-1 \\ -C_i & j = i+1 \\ 0 & \text{otherwise} \end{cases} \tag{36}$$

with $C_0 = C_L$ and $C_N = C_R$, and

$$C_{i\alpha} = -C_L\delta_{i1}\delta_{L\alpha} - C_R\delta_{iN}\delta_{R\alpha} \tag{37}$$

where $C_{\mathrm{g}}^{(i)}$ is the capacitance between dot i and gate electrode.

4. Numerical results for a three-QD system

In this section we present the numerical results for a 1D array of three QDs at equilibrium ($\mu_L = \mu_R$) based on equations (31)–(35). In our numerical calculations we assume that $C_1 = C_2 = C_3 = C_{\mathrm{d}}$, $C_g^{(i)} = C_g$ and $C_L = C_R$, and that there is only one channel in the contacts and one energy level (all equal) in every QD, i.e., $\epsilon_1^0 = \epsilon_2^0 = \epsilon_3^0 = 0$. In addition, the inter-dot tunnel coupling is assumed as $V_{i,i+1} = V$. Since different elements of the conductance have similar properties, we only present the results for the diagonal conductance element $\sigma_{LL}(\omega)$ for discussion. In the wide-band limit, the resonant width Γ_α ($\alpha \in L, R$) are energy-independent constants. Hereafter, all energies are measured in units of $\Gamma = \Gamma_L + \Gamma_R$, frequency in units of $\Gamma/\hbar$, and capacitance in units of e^2/Γ.

First we consider the perfect-screening case [9] ($C_L = C_R = C_{\mathrm{d}} = C_{\mathrm{g}} = 0$). In figure 1 we plot the low-temperature ($T = 0.01$) ac conductance of the three-dot system against the frequency ω for different chemical potentials μ. The inter-dot tunnel coupling is taken as $V = 2$. In figure 1(a) we present the real part of the diagonal admittance $\mathrm{Re}[\sigma_{LL}(\omega)]$ as a function of ω for $\mu = 0, 2$ and $\sqrt{2}V$. The ac conductance at $\omega = 0$ should be equal to the dc conductance. We see that for $\mu = 2$ the curve of $\mathrm{Re}[\sigma_{LL}(\omega)]$ increases as ω increases for small frequency, and exhibits three peaks at $\omega \sim 1$, 2.2, and 4.5. However, for the other two curves $\mathrm{Re}[\sigma_{LL}(\omega)]$ is very large at $\omega = 0$, in contrast to the curve for $\mu = 2$, and decreases rapidly as ω increases from zero frequency. For $\mu = \sqrt{2}V$ and 0 the curves show two small peaks and one peak at $\omega \neq 0$, respectively. This is not surprising; it is a result of the so-called photon-assisted tunnelling that makes the conductance move toward the resonant value when the Fermi level deviates from the resonant energy E_r (here $E_r = 0$, and $\pm\sqrt{2}V$), but for $\mu = 0$ and $\sqrt{2}V$ the Fermi level is right at the resonant energy. According to the Fermi golden rule, the two peaks of $\mathrm{Re}[\sigma_{LL}(\omega)]$ should appear at the frequency $\omega = |E_r - \mu|$. However, as we pointed out in [18], the Fermi golden rule alone cannot explain the behaviour of the current here, because the time-dependent voltages make the effective density of states dependent on the frequency. In other words, in equation (22) the first term accords with the Fermi golden rule, while the other terms do not—they reflect the change of the effective density of states in the dots. So the position of the peaks would deviate from $|E_r - \mu|$, and delay to somewhat

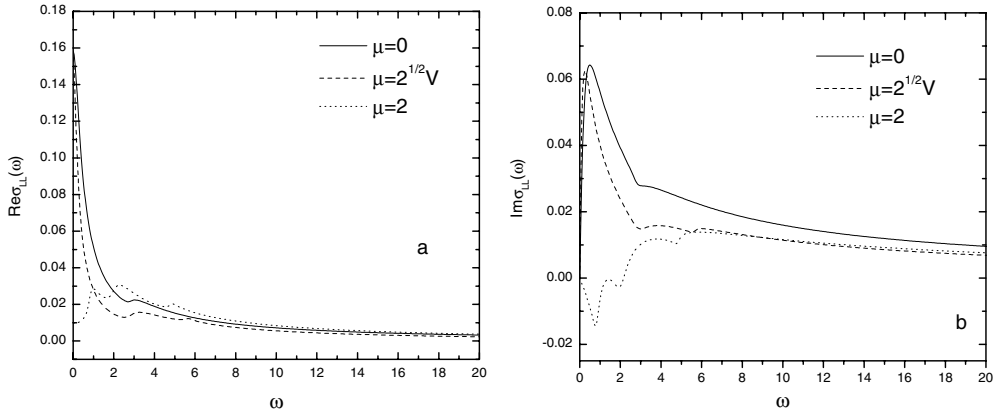

Figure 1. Plots of the real part (a) and imaginary part (b) of the conductance as functions of frequency for a triple-QD system at low temperature ($T = 0.01$). $\epsilon_0 = 0$, $V = 2$. $\mu = 0$ (solid curve), $\sqrt{2}V$ (dashed curve), and 2 (dotted curve). The conductance is measured in units of $e^2/\hbar$, and all energies are in units of $\Gamma = \Gamma_L + \Gamma_R$ where $\Gamma_L = \Gamma_R = 0.5$.

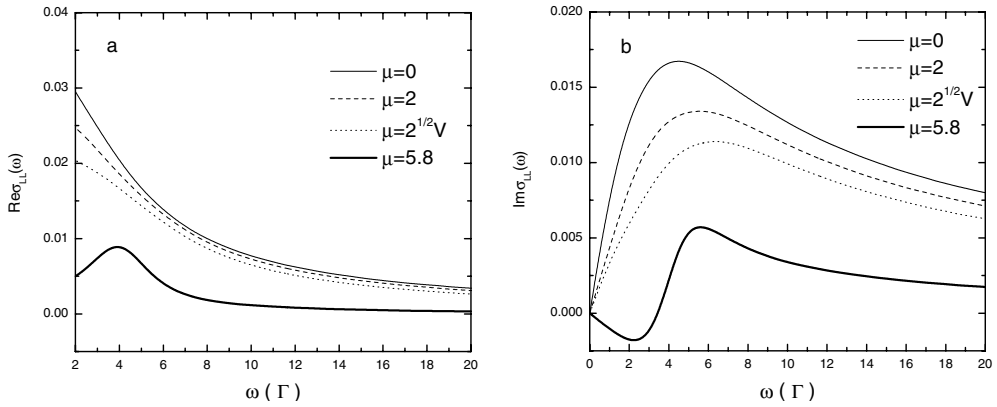

Figure 2. Plots of the real part (a) and imaginary part (b) of the conductance against frequency for a triple-QD system at high temperature ($T = 1$). $\epsilon_0 = 0$, $V = 2$. $\mu = 0$ (solid curve), $\sqrt{2}V$ (dotted curve), 2 (dashed curve), and 5.8 (thick curve). The conductance is measured in units of $e^2/\hbar$, all energies are in units of $\Gamma = \Gamma_L + \Gamma_R$ where $\Gamma_L = \Gamma_R$, and the capacitance is in units of e^2/Γ.

higher frequency. For $\mu = 0$ only one small peak of $\omega \neq 0$ appears; this is because in this case $|\sqrt{2}V - \mu| = |-\sqrt{2}V - \mu|$. We also present the imaginary parts of the diagonal admittance $\mathrm{Im}[\sigma_{LL}(\omega)]$ in figure 1(b). As expected, all curves show $\mathrm{Im}[\sigma_{LL}(0)] = 0$. For the curve for $\mu = 2$, $\mathrm{Im}[\sigma_{LL}(\omega)]$ goes negative from zero when the frequency increases from zero, so the low-frequency conductance shows capacitive behaviour. When $\mu = E_r$, or the frequency is sufficiently high, $\mathrm{Im}[\sigma_{LL}(\omega)]$ is always positive, so the system shows inductive behaviour. However, our calculation shows that for sufficiently large gate capacitance (C_g) and/or lead contact capacitance ($C_{L/R}$), $\mathrm{Im}[\sigma_{LL}(\omega)]$ for low frequency may be negative even if $\mu = E_r$ (see figure 4). This is in agreement with the results of [9] for the single-QD system. For $\mathrm{Im}[\sigma_{LL}(\omega)]$ there are also three resonant frequencies, which are slightly less than $|E_r - \mu|$ if $\mu \neq E_r$.

In figure 2 we present the results for the case of high temperature ($T = \Gamma$) and various chemical potentials. One can see that for $\mu = 0$, 2, and $\sqrt{2}V$ the peak structure disappears.

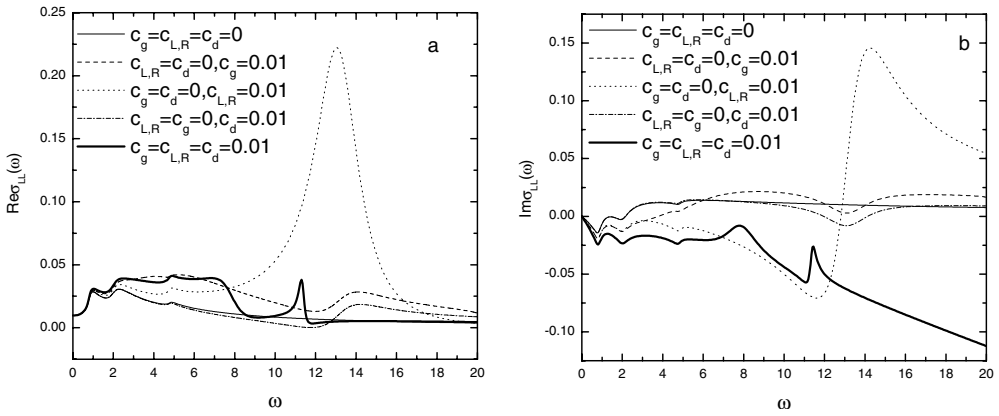

Figure 3. Plots of the real part (a) and imaginary part (b) of the conductance against frequency for a triple-QD system for $\mu = 2$ at low temperature ($T = 0.01$), and in the presence of the capacitances. The other parameters are the same as in figure 1. The conductance is measured in units of $e^2/\hbar$, capacitance in units of e^2/Γ, all energies in units of $\Gamma = \Gamma_L + \Gamma_R$ where $\Gamma_L = \Gamma_R$, and capacitance in units of e^2/Γ.

With increasing frequency, $\mathrm{Re}\,\sigma_{LL}(\omega)$ decreases monotonically, and $\mathrm{Im}\,\sigma_{LL}(\omega)$ is positive for all frequencies. We conclude that for a given μ, when the temperature is sufficiently high the conductance always shows inductive behaviour in the perfect-screening case. However, when $\mu = 5.8$, i.e., the chemical potential is further away from the resonant energy, the peak structure appears again and the imaginary part of the low-frequency conductance is negative (see the thick solid curves). On the other hand, our calculation shows that as in the low-temperature case, a sufficiently large gate capacitance (C_g) and/or lead contact capacitance ($C_{L/R}$) can give rise to a negative $\mathrm{Im}[\sigma_{LL}(\omega)]$ for small frequency, even if $\mu = E_r$.

Next we investigate the effect of the capacitance on the admittance of the three-dot system. First we discuss the behaviour of the frequency-dependent conductance $\sigma_{\alpha\beta}(\omega)$ in the case of small capacitances. In figure 3 we present the results at low temperature ($T = 0.01$), for $\mu = 2$ and different capacitances. For small frequency, all the capacitances have only minor effects on the conductance, especially on the real parts. This is in accord with expectation, because the capacitances have no effect on the dc conductance. With the increase of the frequency the capacitance's influence on the conductance becomes remarkable, and gives rise to some additional peaks. The peaks caused by lead–dot capacitances are the largest. It is interesting to note that the influences of different capacitances on the conductance cancel each other partially for high frequency (see the thick solid curves). In figure 3(b), we see that with the capacitance C_g and $C_{L,R}$ added, the low-frequency parts of the curves of $\mathrm{Im}\,\sigma_{LL}(\omega)$ move downward, keeping $\mathrm{Im}\,\sigma_{LL}(0) = 0$. When the capacitances are added one by one, we find that for low frequency, $\mathrm{Im}\,\sigma_{LL}(\omega)$ moves down monotonically. If we use capacitance values different from 0.01, our calculation shows that with increasing value of the capacitance, for low frequency, $\mathrm{Im}\,\sigma_{LL}(\omega)$ also moves down monotonically. Therefore we conclude that on adding capacitances C_g and $C_{L,R}$ into the system, or increasing the values of the capacitances, the effective capacitance $C_\mathrm{eff} \sim -\mathrm{dIm}\,\sigma_{LL}(0)/\mathrm{d}\omega$ increases, but the inter-dot capacitance C_d has almost no effect on low-frequency admittance.

In figure 4, we present the high-temperature conductances of the system with gate capacitances for different chemical potentials. Comparing with figure 2, one can see that the capacitance has a considerable effect on the frequency-dependent conductance. Due to

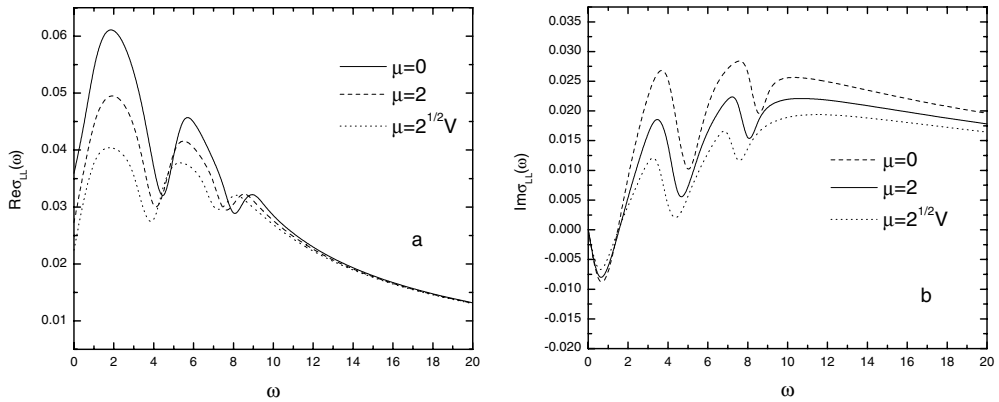

Figure 4. Plots of the real part (a) and imaginary part (b) of the conductance against frequency for a triple-QD system at high temperature ($T = 1$), and in the presence of the capacitances. $\mu = 0$ (solid curve), 2 (dashed curve), and $\sqrt{2}V$ (dotted curve). The other parameters are the same as in figure 2. The conductance is measured in units of $e^2/\hbar$, capacitance in units of e^2/Γ, all energies in units of $\Gamma = \Gamma_L + \Gamma_R$ where $\Gamma_L = \Gamma_R$, and capacitance in units of e^2/Γ.

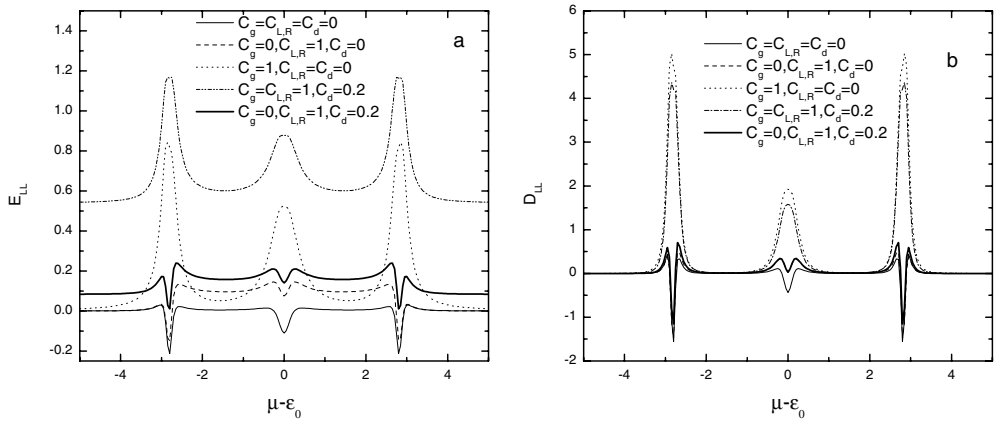

Figure 5. Plots of the diagonal emittance E_{LL} (a) and D_{LL} (b) against chemical potential μ, for a triple-QD system at low temperature ($T = 0.01$), and for various sets of capacitance parameters. Here capacitance and E_{LL} are measured in units of e^2/Γ, D_{LL} in units of $\hbar e^2/\Gamma^2$, and all energies in units of $\Gamma = \Gamma_L + \Gamma_R$ where $\Gamma_L/\Gamma = 0.9$. The other parameters are the same as in figure 1.

the capacitance, the conductance curves show a three-peak structure in both the real and imaginary parts. Our calculations for different 1D arrays also show that at high temperature the number of peaks due to the capacitances is equal to that of QDs in the system. In the three cases (corresponding to three different μ-values), for a given gate capacitance all of the low-frequency conductances are negative, and hence show capacitive behaviour.

To deal with the properties of the low-frequency conductance more effectively, we expand the conductance to second order in frequency:

$$\sigma_{\alpha\beta}(\omega) = \sigma_{\alpha\beta}(0) - \mathrm{i}\omega E_{\alpha\beta} + \omega^2 D_{\alpha\beta} + \mathrm{O}(\omega^3) \tag{38}$$

where $E_{\alpha\beta} = -\mathrm{d}\,\mathrm{Im}[\sigma_{\alpha\beta}(0)]/\mathrm{d}\omega$ is called the emittance, and $D_{\alpha\beta} = \frac{1}{2}\,\mathrm{d}^2\,\mathrm{Re}[\sigma_{\alpha\beta}(0)]/\mathrm{d}\omega^2$. We plot the diagonal emittance element $E_{LL}(\mu)$ and $D_{LL}(\mu)$ for the three-QD system against chemical potential μ in figure 5, for a ratio $\Gamma_L/\Gamma = 0.9$, temperature $T = 0.01$, and

different sets of capacitance parameters. In the case of perfect screening (solid curve) where $C_g = C_{L,R} = C_d = 0$, the low-temperature diagonal emittance is always positive (showing a capacitive behaviour) when the chemical potential μ is far from the resonant energy, but it is negative (showing an inductive behaviour) when the chemical potential is close to the resonant energy. Inductive (negative-maximum) peaks appear at the resonant energies, and two capacitive peaks appear near and on either side of each inductive peak. This accords with the results obtained by Prêtre *et al* [9] for a one-QD system. $D_{LL}(\mu)$ is shown in figure 5(b), and has similar properties to E_{LL} in the case of perfect screening. When temperature increases, both the capacitive and inductive peaks are smoothed and the amplitude of E_{11} decreases rapidly, and the capacitive peaks are pushed further away from resonant energy and the emittance is negative in a larger region around the resonant energy (see figure 2(b)). To show the influence of the capacitances on $E_{LL}(\mu)$ and $D_{LL}(\mu)$, in figure 5 we present the results for different capacitances. The curves for $C_L = C_R = 1$ and $C_g = C_d = 0$ (see the key in the figure) show that there is an increase in E_{LL} and in D_{LL} but more obviously in E_{LL}. The curves for $C_g = 1$ and $C_L = C_R = C_d = 0$ (see the key) show that there is a large increase in both E_{LL} and D_{LL}; in particular, when the chemical potential is close to the resonant energy the negative peaks change to positive peaks. In the figures, we also present the results in the presence of C_d, and find that the effect of inter-dot capacitance C_d is very interesting. When the lead capacitance $C_L = C_R = 0$, the inter-dot capacitance has no obvious influence on either E_{LL} or D_{LL}. However, when $C_L = C_R \neq 0$, the inter-dot capacitance has a considerable effect on E_{LL}, making the whole $E_{LL}(\mu)$ curves shift upward (see the dash–dotted curve and the thick curve in figure 5(a)), but it does not have a similar effect on D_{LL} (see figure 5(b)). In addition, our calculation indicates that for Γ_L there are two critical values, $\Gamma_L^{c,E}$ and $\Gamma_L^{c,D}$, below which $E_{LL}(\mu)$ and $D_{LL}(\mu)$ at resonant energies are always negative, and the critical values depend on the temperature.

5. Conclusions

In summary, we have presented a general approach for calculating the dynamical conductance of the tunnel-coupled QD arrays. To consider the long-range Coulomb interaction, we have introduced the geometrical capacitances between the leads and dots, gate electrode and dots, and dots and dots. The displacement currents are also considered. The internal time-dependent potentials in the dots are determined self-consistently. As a result, our results fulfil the charge and current conservation requirement, as well as the current and charge invariance under an overall potential shift. Applying our approach to a 1D QD array, we have given the formulae for calculating the frequency-dependent conductance and charge response by using the non-equilibrium Green function techniques. Numerical calculation of the ac conductance has been carried out for a coupled three-QD system. The three-peak resonant structure of the ac conductance is observed at low temperature, but it disappears at high temperature. We have also studied the effect of the capacitance on the frequency-dependent conductance and found that even small capacitances have a considerable effect on the frequency dependence of the conductance, but they have a very small effect on the low-frequency conductance, especially on the real parts. However, except for the inter-dot capacitance, the small capacitances have a slight but non-negligible effect on the imaginary part of the low-frequency conductance for the chemical potential far from resonant energy. For high frequency all the capacitances have a considerable effect on the ac conductance. Finally, we calculated the low-frequency conductance as a function of the chemical potential. The low-frequency conductance shows either capacitive or inductive behaviour depending on the value of the chemical potential, but sufficiently large capacitances can change this situation.

References

[1] Kouwenhoven L P, Jauhar S, Orenstein J and McEuen P L 1994 *Phys. Rev. Lett.* **73** 3443
Blick R H, Hang R J, van der Weide D W, von Klitzing K and Eherl K 1995 *Appl. Phys. Lett.* **67** 3924
[2] Oosterkamp T H, Kouwenhoven L P, Koolen A E A, van der Vaart N C and Harmans C J P M 1997 *Phys. Rev. Lett.* **78** 1536
Oosterkamp T H, Kouwenhoven L P, Koolen A E A, van der Vaart N C and Harmans C J P M 1998 *Nature* **395** 873
[3] Geerligs L J, Anderegg V F, Holweg P A M, Mooij J E, Pothier H, Esteve D, Urbina C and Devoret M H 1990 *Phys. Rev. Lett.* **64** 2691
[4] Jauho A-P, Wingreen N S and Meir Y 1994 *Phys. Rev.* B **50** 5528
[5] Anantram M P and Datta S 1995 *Phys. Rev.* B **51** 7632
[6] Goldlin Y and Avishai 2000 *Phys. Rev.* B **61** 16 750
[7] Bruder C and Schoeller H 1994 *Phys. Rev. Lett.* **72** 1076
[8] Ziegler R, Bruder C and Schoeller H 2000 *Phys. Rev.* B **62** 1961
[9] Büttiker M, Prêtre A and Thomas H 1993 *Phys. Rev. Lett.* **70** 4114
Prêtre A, Thomas H and Büttiker M 1996 *Phys. Rev.* B **54** 8130
[10] Christen T and Buttiker M 1996 *Phys. Rev.* B **53** 2064
[11] Büttiker M and Martin A M 2000 *Phys. Rev.* B **61** 2737
[12] Anantram M P and Roychowdhury V P 1999 *J. Appl. Phys.* **85** 1622
[13] Stafford C A and Wingreen N S 1996 *Phys. Rev. Lett.* **76** 1916
[14] Ivanov T 1997 *Phys. Rev.* B **56** 12 339
[15] Ma Z, Shi J and Xie X C 2000 *Phys. Rev.* B **62** 15 352
[16] Au-Yeung T C, Shangguan W Z, Chen Q H, Yu Y B, Kam C H and Wongand M C 2002 *Phys. Rev.* B **65** 035306
[17] Yu Y B, Au Yeung T C, Shangguan W Z and Cham C H 2000 *Phys. Lett.* A **275** 131
[18] Yu Y B, Au Yeung T C, Shangguan W Z and Kam C H 2001 *Phys. Rev.* B **63** 205314
[19] Shangguan W Z, Au Yeung T C, Yu Y B and Kam C H 2000 *Phys. Rev.* B **63** 235323
[20] Livermore C, Crouch C H, Westervelt R M, Campman K L and Gossard A C 1996 *Science* **274** 1332
[21] Schedelbeck G, Wegscheider W, Bichler M and Abstreiter G 1997 *Science* **278** 1792
[22] Andresen A *et al* 1999 *Phys. Rev.* B **60** 16 050
[23] Lin L H *et al* 1999 *Phys. Rev.* B **60** R16 299
[24] Duruöz C I, Clarke R M, Marcus C M and Harris J S 1995 *Phys. Rev. Lett.* **74** 3237
[25] Wang K H, Pecher A, Höfling E and Forchel A 1997 *J. Vac. Sci. Technol.* B **15** 2829